

Film mulching can alleviate soil quality decrease and produce high maize yield under different irrigation strategies

Hao Quan^{a,b}, Lihong Wu^{a,b}, Jiaming Sun^{a,b}, Tibin Zhang^{b,c}, Lianhai Wu^d, Kadambot H.M. Siddique^e, Hao Feng^{b,c,*}, Bin Wang^{f,**}

^a College of Water Resources and Architectural Engineering, Northwest A&F University, Yangling, Shaanxi 712100, China

^b State Key Laboratory of Soil Erosion and Dryland Farming on the Loess Plateau, Institute of Soil and Water Conservation, Northwest A&F University, Yangling 712100, China

^c Institute of Soil and Water Conservation, Chinese Academy of Sciences and Ministry of Water Resources, Yangling, Shaanxi 712100, China

^d Sustainable Agriculture Sciences, Rothamsted Research, North Wyke, Okehampton, Devon EX20 2SB, UK

^e The UWA Institute of Agriculture, The University of Western Australia, Perth, WA 6001, Australia

^f NSW Department of Primary Industries, Wagga Wagga Agricultural Institute, NSW 2650, Australia

ARTICLE INFO

Handling Editor - J.E. Fernández

Keywords:

Irrigation strategy
Plastic film
Maize yield
Soil quality index
Water and nitrogen use

ABSTRACT

Plastic film mulching (PM) combined with irrigation is widely adopted to improve crop yields, water and nitrogen efficiency, especially in arid farming areas. Despite its benefits, the effects of this method on soil quality and its subsequent impact on crop productivity and resource efficiency have not been thoroughly investigated. In this study, we formulated a soil quality indicator (SQI) from five years of field experiments in the Hetao Irrigation District (HID) of Northwestern China. The treatments included border irrigation as the control treatment (CK), CK combined with PM (BI_{PM}), and three water level drip irrigation treatments combined with PM. Three threshold values of soil matric potential for drip irrigation were -10 kPa (HDI_{PM}), -30 kPa (MDI_{PM}), and -50 kPa (LDI_{PM}). We then examined the SQI changes based on measured multiple soil properties and assessed their implications for maize yield, irrigation water productivity (IWP), and partial factor productivity of nitrogen (PFPN). We found: (1) from 2016 to 2020, HDI_{PM} achieved the highest average yield (15.77 t ha⁻¹), IWP (3.73 kg m⁻³), and PFPN (63.18 kg kg⁻¹), showing increases of 54.77 %, 84.90 %, and 96.93 % over the control treatment, respectively; (2) no significant variations in the SQI were observed for HDI_{PM} in 2020 in the topsoil (0–30 cm) and subsoil (30–60 cm) compared to the initial condition. However, CK, BI_{PM}, MDI_{PM}, and LDI_{PM} showed reductions in SQI in both soil layers, primarily due to decreased soil organic carbon (SOC) and structural stability, along with increased sand content and soil salinity; (3) according to the linear mixed-effects model, a low SQI (< 0.43), elevated temperatures, and drought indices negatively impact yield. Hence, we advocate for HDI_{PM} to maximize yield and PFPN. To enhance soil quality, identifying agronomic practices that increase SOC and reduce soil salinity in the HID is crucial.

1. Introduction

Soil plays a pivotal role in agricultural ecosystems, offering vital functions that support plant growth and productivity. These include nutrient and water cycling, decomposition of litter and residues, variations in soil carbon, and greenhouse gas emissions (Seconda et al., 2021; Vasu et al., 2016). A healthy soil system is fundamental to ensuring global food security and plays a crucial role in mitigating global warming and reducing agricultural pollution (Foley et al., 2011; Qiao

et al., 2022). Yet, over one-third of the world's soils are currently facing moderate to severe degradation, a condition primarily attributed to intensive farming practices and a deficiency in conservation efforts (Rojas et al., 2016).

In the Hetao Irrigation District (HID) of China, the overuse of chemical fertilizers and irrigation water has been shown to deteriorate soil structure, induce secondary salinization at the surface, and contaminate groundwater (Wang et al., 2020b). Meanwhile, the high salinity of the soil in the HID region leads to a high concentration of soil

* Correspondence to: Institute of Soil and Water Conservation, Northwest A&F University, Yangling, Shaanxi 712100, China.

** Corresponding author.

E-mail addresses: nercwsj@vip.sina.com (H. Feng), bin.a.wang@dpi.nsw.gov.au (B. Wang).

<https://doi.org/10.1016/j.agwat.2024.109221>

Received 10 March 2024; Received in revised form 27 November 2024; Accepted 3 December 2024

Available online 5 December 2024

0378-3774/© 2024 The Author(s). Published by Elsevier B.V. This is an open access article under the CC BY license (<http://creativecommons.org/licenses/by/4.0/>).

solution, reducing soil water potential and thereby inhibiting key physiological activities in crops, such as stomatal closure and photosynthesis reduction (Munns and Tester, 2008). Soil salinization can also affect soil pore structure and hinder water infiltration (Feng et al., 2024; Salcedo et al., 2022). Additionally, the scarcity of organic material applications has been linked to a gradual reduction in soil organic carbon (SOC) levels (Yang et al., 2020). The practice of combining film mulching with irrigation, widely recognized for its ability to improve soil moisture and boost crop yields (Guo et al., 2021; Zhang et al., 2021), is particularly valuable in arid irrigation areas for enhancing soil water and nutrient conditions, thus supporting stable crop production. However, the long-term use of film mulching is associated with several negative impacts, including decreased soil porosity and pH (Wang et al., 2017), salt accumulation at the soil surface (Li et al., 2019), and increased SOC mineralization risk, which hastens SOC depletion (Zhang et al., 2022a). After long-term use of plastic film, fragments enter and remain in the soil, where they are termed residual film. Residual film on the farm reduces nutrient supply to crops and microbial species, inhibiting the activities of soil microorganisms (Qi et al., 2020). It also disrupts soil structure, reduces soil permeability, and inhibits root development (Gao et al., 2019; Jiang et al., 2017). Consequently, while film mulching meets immediate crop growth requirements, it also poses a significant risk of soil degradation, challenging its viability as a sustainable high-yield strategy. Therefore, analyzing soil property changes resulting from the combination of film mulching and irrigation is essential for evaluating soil quality and fostering sustainable practices in irrigated agriculture.

The soil quality indicator (SQI) is commonly utilized to evaluate changes in soil quality by integrating multiple indices (Zhang et al., 2020). For instance, Nunes et al. (2020) employed soil management assessment framework scoring algorithms to derive a SQI, amalgamating essential soil data for evaluating soil health under various tillage practices. Similarly, Luo et al. (2017) determined SQI at different soil depths, revealing that higher SQI values are associated with increased yields. Despite such progress, comprehensive studies on the long-term effects of film mulching on soil quality, especially concerning the simultaneous analysis of diverse physical and chemical soil properties, remain scarce. Previous research has typically focused on assessing specific soil attributes in the context of film mulching (Yang et al., 2023; Zhao et al., 2023), leaving a significant gap in understanding its overall impact on soil quality during continuous maize cultivation. Additionally, although film mulching can potentially enhance soil nutrient availability by modifying soil moisture and temperature environment, thereby increasing yields (Quan et al., 2022), a quantitative correlation between SQI and yield, specifically within the context of film mulching, remains to be established.

Research methods to understand the dynamics between environmental factors (weather, crops, and soil) and crop yield have diversified. For example, Li et al. (2021) applied the random forest technique to predict yields using comprehensive datasets, including weather conditions, vegetation indices, and soil characteristics, highlighting the importance of radiation and soil moisture at key growth stages as yield determinants. De Cárcer et al. (2019) employed a multiple linear regression model, integrating canopy temperature, soil moisture, and drought-related indices to estimate yields. Similarly, Zhang et al. (2022b) investigated how soil properties such as organic matter and pH, along with crop growth metrics like leaf nitrogen content and height, influence maize biomass using machine learning to assess factor contributions. Despite these advances, comprehensive yield prediction considering a broad range of soil properties and climatic variables, especially under prolonged film mulching and irrigation regimes, is scarce. The comprehensive analysis of soil quality dynamics and the identification of yield-limiting factors under film mulching represent a research domain that has not been thoroughly investigated.

The HID, located in northwest China, is a key arid irrigated region producing over 3.0 million tons of maize annually. However, the

region's agricultural development, marked by expanded cropland and intensive practices such as excessive irrigation and fertilization, has contributed to declining soil quality, adversely affecting spring maize production (Meng et al., 2017). In this study, we hypothesized that the combination of mulching and drip irrigation could alleviate the negative effects of soil quality decline on maize yield, as well as water and nitrogen efficiency, due to the favorable soil water environment created by this combination. We aimed to: (1) determine the optimal combination of film mulching and irrigation techniques that maximizes yield, as well as water and nitrogen use efficiencies over a five-year continuous field experiment; (2) assess the impact of integrating film mulch with effective irrigation methods on soil quality; and (3) establish the SQI threshold that affects maize yield by quantifying the correlation between SQI and maize yield.

2. Materials and methods

2.1. Experimental site description

A field experiment spanning five years (2016–2020) was carried out at the Shuguang Irrigation Research Station, located in the HID, Inner Mongolia Autonomous Region, China (latitude 40°43'N, longitude 107°13'E, altitude 1039 m). Shuguang site, characterized by an arid climate, experiences an average air temperature of 21.8°C and an average annual precipitation of 90.8 mm during the maize cultivation season, according to data from a weather station located approximately 200 m from the study site. The soil at the study site was classified as silt loam in the top layer (0–60 cm) and sandy loam in the 60–90 cm layer (USDA soil textural triangle). Detailed physicochemical properties of the soil at Shuguang are documented in Table 1. Initial soil conditions in 2016 for the 0–60 cm layer reported average SOC at 4.31 g kg⁻¹, total nitrogen (TN) levels of 110.5 mg kg⁻¹, available phosphorus (AP) at 52.8 mg kg⁻¹, and available potassium (AK) at 132.6 mg kg⁻¹.

Weather parameters such as rainfall, temperature, relative humidity, wind speed, and radiation were automatically logged on an hourly basis by an automated meteorological station (HOBO, Campbell Scientific Inc., USA), located approximately 500 m from the experiment near the field site and stored in a data logger for later extraction of daily mean values. The groundwater level from 2016–2020 ranged from 1.2–3.5 m.

2.2. Experimental design

The study was structured using a block split-plot design, incorporating two primary irrigation methods (border irrigation and drip irrigation) as the main blocks. The border irrigation subplots included border irrigation without film mulching, which served as the control (CK), while border irrigation combined with film mulching (BI_PM) served as a comparison. The drip irrigation subplots were determined by soil matric potential at a depth of 20 cm below the drip lines: –10 kPa (high soil matric potential under PM, HDI_PM), –30 kPa (medium soil

Table 1
Physicochemical properties at the experimental site before sowing in 2016.

Soil layers (cm)	Soil texture	Soil bulk density (g cm ⁻³)	Field capacity (cm ³ cm ⁻³)	Ks (cm h ⁻¹)	ECe (dS m ⁻¹)	pH	SOC (g kg ⁻¹)
0–30	Silt loam	1.38	0.30	0.14	7.08	8.5	4.98
30–60	Silt loam	1.40	0.31	0.12	4.14	8.2	3.64
60–90	Sandy loam	1.50	0.22	25.14	2.80	8.3	3.78
90–120	Silt loam	1.42	0.29	4.70	2.33	8.1	3.58

Note: Ks, saturated hydraulic conductivity; ECe, electrical conductivity of saturated extract; SOC, soil organic carbon.

matric potential under PM, MDI_PM), and -50 kPa (low soil matric potential under PM, LDI) with PM. Thus, our experiment included a total of five treatments: CK, BI_PM, HDI_PM, MDI_PM, and LDI_PM. Consequently, the experiment had five treatments with three replicates (15 plots). The soil matric potential used to trigger drip irrigation was measured using a tensiometer, which was installed at a depth of 20 cm below the drip emitter and read daily at 8:00 am and 3:00 pm. Each plot ($12\text{ m} \times 4\text{ m}$), comprising eight rows of maize, was surrounded by 15 cm high ridges to avoid runoff, with 2 m between plots to minimize lateral infiltration of irrigation water.

2.3. Field management practices

All treatments (except CK) utilized transparent film mulching (0.010 mm thick, with an albedo of 0.11), achieving a mulch area ratio of 0.7. For the drip irrigation treatments, the drip emitters, positioned beneath the transparent film, were arranged at intervals of 30 cm along a drip irrigation line, with an irrigation volume of 2.5 L h^{-1} and water pressure of 0.1 MPa. The spacing between drip lines is 1 m for drip irrigation treatments (Fig. S1).

Maize seeds of the variety 'Ximeng 6' were sown at a depth of 5 cm using a hole-sowing machine, subsequent to film application. Each plastic film sheet accommodated two maize rows, spaced 40 cm apart, with an inter-plant distance of 30 cm, achieving a planting density of 6.7 plants m^{-2} . Sowing dates spanned April 27, 2016; April 28, 2017; April 29, 2018; April 28, 2019; and April 29, 2020, with corresponding harvest dates of September 9, 2016, September 8, 2017, September 10, 2018, September 8, 2019, and September 9, 2020. All fields were left fallow after the maize harvest. After the maize harvest, the residue was removed from the plot. After that, autumn irrigation was carried out each November in the studied field to reduce soil salinity.

The CK and BI_PM treatment adhered to established local irrigation practices, distributing the total irrigation volume equally across the four pivotal maize growth stages: 6-leaf (V6), 12-leaf (V12), tasseling (VT), and grain filling (R3). For the drip irrigation treatments, irrigation was applied whenever the soil matric potential reached predetermined threshold values. Detailed irrigation schedules are outlined in Table S1. Throughout the five-year study period, the irrigation water maintained a pH of 7.86 and soil electrical conductivity of the extracted solution (ECe) of 1.76 dS m^{-1} .

Prior to sowing, a basal application of NPK fertilizer—comprising 163 kg ha^{-1} of urea, 420 kg ha^{-1} of diammonium phosphate, and 90 kg ha^{-1} of potassium sulfate—was evenly spread in each plot and incorporated into the soil through rotary tillage to a depth of 20 cm each season. For the CK and BI_PM treatments, topdressing with 326 kg ha^{-1} of urea was mixed with irrigation water at the R3 and subsequently irrigated. The drip irrigation treatments received topdressing through a combined irrigation and fertilization system during scheduled irrigation events (Table S2). These agronomic practices were consistently applied each year. Adhering to local agricultural standards, field management also involved regular weeding and pesticide application to control insects.

2.4. Field data collection and relevant indexes calculation

2.4.1. Soil properties indexes

Soil samples, both disturbed and undisturbed, were collected annually at the end of the experiment, from depths of 0–60 cm in 10 cm increments, with each treatment having five replicates. Composite samples for both topsoil (0–30 cm) and subsoil (30–60 cm) were prepared by homogenizing individual soil samples. These were then securely sealed in plastic bags for transport to the laboratory. The undisturbed samples facilitated the calculation of dry soil bulk density (BD) and total porosity (SP) using formula (1) based on Teixeira et al. (2017). Soil water content (SWC) was assessed through the oven-drying method at 105°C for 24 hours. Specifically, soil volumetric water content was

calculated by multiplying the gravimetric water content by the bulk density (Ma et al., 2023). Field capacity (FMC) and saturated hydraulic conductivity (K_s) were evaluated using the standard method established by Klute and Dirksen (1986). Disturbed soil samples were used to determine soil particle size distribution as per Teixeira et al. (2017).

Soil basic chemical properties were analyzed following the methodologies described by Bao (2000). SOC values were assessed using the wet oxidation technique (Nelson and Sommers, 1982). TN concentrations were measured via the Kjeldahl method. The concentration of soil nitrate-nitrogen ($\text{NO}_3\text{-N}$) and soil ammonium-nitrogen ($\text{NH}_4^+\text{-N}$) in potassium chloride (KCl) extract samples were determined with a micro-flow AutoAnalyzer3 (AA3, SEAL Company, Germany). AP was quantified using the 0.5 M NaHCO_3 extraction followed by the molybdenum antimony sulfate colorimetric method, while AK was extracted with 1 M ammonium acetate (NH_4OAc) and measured through flame photometry. The pH of the soil was evaluated with a 1:2.5 soil-to-water ratio (w/v) using a pH meter (PHS-3C, REX, Shanghai, China). Soil electrical conductivity ($\text{EC}_{1:5}$) in the extract solution was recorded using a DDS-307A conductivity meter (Shanghai Rex Instrument, China) after a 1:5 soil-water mixture. ECe was calculated using formula (2) (Dong et al., 2018; Qi et al., 2018; Tong et al., 2015). Lastly, the structural stability index (SSI) was computed using formula (3) to evaluate the risk of soil degradation, according to Pieri (1992).

$$SP = [1 - BD / \text{soil particle gravity}] \times 100 \quad (1)$$

where SP is total soil porosity (%), BD is soil bulk density (g cm^{-3}), and soil particle gravity is the standard value of 2.65 g cm^{-3} .

$$\text{ECe} = 1.33 + 5.88 \times \text{EC}_{1:5} \quad (2)$$

where $\text{EC}_{1:5}$ is the electrical conductivity of the soil extract solution (dS m^{-1}) and ECe is the electrical conductivity of the saturated extract (dS m^{-1}).

$$\text{SSI} = \left[\frac{\text{SOM}}{\text{Clay} + \text{Silt}} \right] \times 100 \quad (3)$$

where SSI (%) is the structural stability index, SOM (%) is soil organic matter content, and Clay+Silt (%) is the combined silt and clay content of the soil.

2.4.2. Crop phenotype indexes and grain yield

At five critical growth stages (V6, V12, VT, R3, and maturity), three uniformly developed plants were destructively sampled from the center of each plot, minimizing edge effects. The leaf area was calculated using the formula: leaf length \times maximal width \times 0.75 (Montgomery, 1911), and the leaf area index (LAI) was subsequently derived by dividing the total leaf area by the plot's surface area. Plant height (PH) was determined using a ruler, whereas stem thickness (ST) was accurately measured with a digital vernier caliper to the nearest 0.001 mm. For aboveground biomass (AGB), the samples were initially dried at 105°C for 30 minutes, followed by at 75°C to constant. During harvest, 15 grains from each of 15 randomly selected plants per plot were collected to evaluate maize harvest factors. These harvested samples were then sun-dried, threshed, and their weight recorded.

2.4.3. Drought indexes calculation

Plant Available Water (PAW) is recognized as a key indicator of plant water stress and is instrumental in assessing the impact of moisture stress on maize yields (Sadras and Milroy, 1996). Research indicates that when PAW falls below 60 % of the Plant Available Water Holding Capacity (PAWC), critical functions such as stomatal conductance, leaf area expansion, and photosynthesis rates experience reductions at various growth stages of maize (Ma et al., 2018). This threshold marks the onset of drought conditions, defined when soil PAW within the root zone (0–100 cm depth) below 60 % PAWC. Drought events are

characterized by their frequency, duration, and intensity: Drought frequency (DF) calculates the total number of drought days across growth stages; drought duration (DD) identifies the longest continuous period of drought within these stages; and drought intensity (DI) measures the severity of soil PAW depletion beyond the drought threshold during these stages.

DF is calculated as follows:

$$DF = \frac{\sum_{j=1}^N m_j}{G_e - G_s + 1}, \quad j = 1, 2, \dots, N, \quad N \geq 1 \quad (4)$$

where G_e and G_s are the start and end of different growth stages (V6, V12, VT, R3, maturity, and the entire growth period), and m_j is the duration of the j th drought event at the same growth stage.

DI is calculated as follows, according to (Li et al., 2023):

$$DI_{ij} = \frac{\delta \times PAWC - PAW_{ij}}{\delta \times PAWC}, \quad j = 1, 2, \dots, m_j; j = 1, 2, \dots, N \quad (5)$$

$$DH_j = \frac{\sum_{i=1}^{m_j} DI_{ij}}{m_j}, \quad j = 1, 2, \dots, N \quad (6)$$

$$DI = \frac{\sum_{j=1}^N DH_j}{N}, \quad j = 1, 2, \dots, N, \quad N \geq 1 \quad (7)$$

where DI_{ij} is the drought intensity on the i th day of the j th drought event at different growth stages, $\delta \times PAWC$ is the threshold to identify drought events, δ is the constant set at $\delta = 0.6$ (Ma et al., 2018), PAW_{ij} is plant available water on the i th day of the j th drought event, and DH_j is the drought intensity for the j th drought event at different growth stages.

2.4.4. Accumulated growth degree days, SOC storage, and water and nitrogen use efficiencies

Accumulated growth degree days (AccuTem, °C day) during the entire season was calculated as follows (Ding et al., 2019):

$$AccuTem = \frac{T_{max} + T_{min}}{2} - T_{base} \quad (8)$$

where T_{max} and T_{min} are the measured daily maximum and minimum air temperatures from the weather station, and T_{base} is maize base temperature (10°C). For $T_{max} > 30^\circ\text{C}$, it was set to 30°C and for $T_{min} < 10^\circ\text{C}$, it was set to 10°C.

The stocks of SOC at topsoil and subsoil were calculated as follows (Luo et al., 2015):

$$SOC_{storage} = C \times BD \times H \times 10 \quad (9)$$

where $SOC_{storage}$ is the storage of SOC (t ha^{-1}), C is the concentration of SOC (g kg^{-1}), BD is the soil bulk density (g cm^{-3}), H is the soil depth (m), and 10 is the unit conversion factor.

Irrigation water productivity (IWP, kg m^{-3}) was expressed as (Rodrigues, Pereira, 2009; Fernández et al., 2020):

$$IWP = \frac{Y}{I \times 10} \quad (10)$$

where Y is yield (kg ha^{-1}) and I is irrigation amount (mm).

The partial factor productivity of nitrogen (PFPN) was calculated (Quan et al., 2022):

$$PFPN = \frac{Y}{F} \times 100\% \quad (11)$$

where Y is yield (kg ha^{-1}) and F is applied nitrogen fertilizer amount (kg ha^{-1}).

2.5. Soil quality indicator calculation

The calculation of the SQI unfolded in three stages. Initially, the Minimum Data Set (MDS) selection was based on its significance in influencing crop yield, soil health, and water availability (Amgain et al., 2022; Gan et al., 2024). Principal Component Analysis (PCA) served to pinpoint relevant indicators within the comprehensive soil property dataset, focusing on variables with significant eigenvalues (≥ 1) and which represented at least 5% of the variance in the data. Subsequently, Pearson's correlation analysis aimed to eliminate redundant variables; in instances where multiple variables within a PC were highly correlated ($r > 0.7$), only the variable with the highest factor loading was retained.

The second step used a linear scoring formula to eliminate the effect of measurement and variable units for soil property indexes. The 'less is better' function (Eq. (12)) (Amgain et al., 2022) was used for the sand property, while the 'more is better' function (Eq. (13)) was used for the other indexes.

$$Y = (X - L)/(H - L) \quad (12)$$

$$Y = 1 - (X - L)/(H - L) \quad (13)$$

where Y indicates the linear score within the range of 0–1, X indicates the soil quality value, L indicates the minimum value, and H indicates the maximum value.

The third step integrated the soil property characteristics into the SQI calculation using the weighted-additive method (Eq. (14)) described by Karlen et al. (1998). In this method, each soil property index within the MDS was calculated through multi-linear regression (MLR) analysis. Within the MLR framework, maize yield was the dependent variable, whereas the soil property indices acted as independent variables. The weight assigned to each index was computed based on the proportion of its standardized regression coefficient relative to the aggregate of standardized regression coefficients for all indices within the MDS.

The chosen soil property indexes in the MDS were used to calculate the weighted-additive SQI (Amgain et al., 2022):

$$SQI = \sum_{i=1}^n WiSi \quad (14)$$

where n is the number of indicators integrated into the MDS, Wi is the weighting factor for soil indexes based on the standardized regression coefficient of each soil property index/the sum of the standardized regression coefficients of all property indexes in MDS, and Si is the SQI score of i th soil property indexes in MDS.

2.6. Model development

2.6.1. Feature selection

To estimate crop AGB and yield, we utilized 17 variables listed in Table 2 as potential predictors. A nonlinear genetic algorithm (GA) approach, as detailed by Welikala et al. (2015), was employed to select the most informative predictors. This method initiates with generating a random initial population, followed by the selection of new individuals to generate solutions (offspring) according to predetermined fitness functions. These offspring then replace the previous generation, aiming to enhance the model's accuracy by reducing the root mean square error through key genetic operations: crossover and mutation. The iterative evolutionary process persists until the search procedure concludes. Following Welikala et al.'s (2015) guidelines, we set the GA parameters to a population size of 50, a crossover rate of 0.8, and a mutation rate of 0.1. The 'Caret' package in R software facilitated the specific feature selection process, targeting crop AGB and yield, with additional variables serving as inputs.

2.6.2. Linear mixed-effects model (LMM)

The LMM for estimating crop AGB and yield incorporated variables

Table 2
Seventeen variables were used to predict aboveground biomass and yield in this study.

Variables	Definition	Unit
<i>Climate</i>		
AveTmax/ AveTmin	Average maximum/minimum daily air temperature at different growth stages/entire growth period	°C
AveTem	Average daily air temperature at different growth stages/entire growth period	°C
AveWind	Average daily wind speed at different growth stages/entire growth period	m s ⁻¹
AveRH	Average daily relative humidity at different growth stages/entire growth period	%
AccuPre	Accumulative daily precipitation from sowing to different growth stages/total accumulation values during the entire growth period	mm
AccuRad	Accumulative daily input radiation from sowing to different growth stages/total accumulation values during the entire growth period	MJ m ⁻² day ⁻¹
T30	Accumulative high-temperature days (>30°C) at different growth stages/total accumulation values during the entire growth period	day
<i>Crop</i>		
AccuTem	Accumulative growth degree days from sowing to different growth stages/total accumulation values during the entire growth period	°C day
LAI	Plant leaf area index at different growth stages/maximum value during the entire growth period	–
PH	Plant height at different growth stages/maximum value during the entire growth period	cm
ST	Plant stem thickness at different growth stages/maximum value during the entire growth period	mm
<i>Management</i>		
DF	Drought event frequency at the different growth stages/total accumulation values during the entire growth period	–
DD	Drought event duration at the different growth stages/total accumulation values during the entire growth period	day
DI	Drought event intensity at the different growth stages/maximum value during the entire growth period	–
<i>Soil quality</i>		
SQITOP/ SQISUB	Soil quality indicator in topsoil/subsoil	–

related to weather, crop phenotypes, management practices, and SQIs. The methodology is depicted in Fig. 1. Initially, a Pearson's correlation analysis was employed to identify predictor variables that exhibited a significant correlation with the target variables ($|r| > 0.3$ and $p < 0.05$). Subsequently, a Variable Inflation Factor (VIF) analysis was conducted to evaluate potential multi-collinearity among the predictors. All predictor variables in the LMM model were statistically independent of each other ($VIF < 10$).

One-way ANOVA was conducted at a significance level of 5% ($p < 0.05$) using the LMM of the lme4 package through restricted maximum likelihood estimation (REML) in R software. Tukey's post hoc test was used to determine the significance between treatments. The LMM was fitted using the 'lmer' function from the 'lme4' package to evaluate the influence of climate, soil, and crop phenotype on maize aboveground biomass and yield.

The specific predictor variable response formula was as follows:

$$y = X\beta + Zu + \varepsilon \quad (15)$$

where y is the AGB (yield) vector (t ha⁻¹), X and β are the design matrix and vectors of fixed effects, respectively, Z and u are the design matrix and vectors of random effects, respectively, and ε is the vector experiment error. The experimental year was the random effect factor. The GA algorithm selected the fixed effects, including weather, crop phenotypes, drought indexes, and SQL. The Relaimpo package in R version 4.1.3 was used to compute relatively important variables and the proportional

contribution of predictor variables to explain the variance in the LMM model.

2.6.3. Variable importance based on random forest model

Recognized for its widespread application in agricultural research, the random forest (RF) model excels in tasks ranging from estimating crop evapotranspiration to yield prediction (Li et al., 2021). Introduced by Breiman (2001), the RF model operates as a tree-based machine learning technique that consolidates multiple decision trees to enhance the accuracy of predictions. To gauge the significance of each predictor within the RF framework, the '%IncMSE' metric was utilized, assessing the relative impact of predictor variables on model performance. Furthermore, Partial Dependence Plots (PDP) were applied to elucidate the specific influence of predictor variables on the target outcome within the RF model. These plots reveal the nature of the relationship—whether linear, monotonic, or complex—between predictor and response variables. The analysis involving PDP and variable importance was executed in R, leveraging the capabilities of the 'randomForest' and 'pdp' packages.

2.6.4. Model evaluation

The performance of the LMM model was evaluated using two statistical indicators—root mean square error (RMSE) and coefficient of determination (R^2). R^2 indicates the fitness of the LMM model for predicting yield, and RMSE measures the distance between the predicted and observed values. A high R^2 value and low RMSE value indicate better estimation accuracies of the model. The formulas used were as follows:

$$R^2 = \frac{[\sum_{i=1}^n (O_i - \bar{O}) \times (S_i - \bar{S})]^2}{\sum_{i=1}^n (O_i - \bar{O})^2 \times \sum_{i=1}^n (S_i - \bar{S})^2} \quad (16)$$

$$RMSE = \sqrt{\frac{1}{n} \sum_{i=1}^n (S_i - O_i)^2} \quad (17)$$

where S_i and O_i are simulated and measured yields, respectively, and \bar{S} and \bar{O} are mean simulated and measured yields, respectively.

3. Results

3.1. Soil properties variation over five years

Most soil samples were alkaline, with a mean pH of 8.60 (range 7.73–9.56) and coefficient of variation (CV) of 4.41 (Table 3). The SOC ranged from 0.32–0.46%, likely due to the practice of continuous cropping without the addition of organic materials. NO₃-N and AP had mean values of 5.99 mg kg⁻¹ and 4.73 mg kg⁻¹, marking them as the soil properties with the highest CV values (Table 3). In addition, the soil had a high silt content (66.81%) and salinity content (mean ECe 6.90 dS m⁻¹).

PCA identified nine critical soil indices—clay content, sand content, BD, SOC, SWC, ECe, pH, NH₄⁺-N, and SSI—in both topsoil and subsoil as integral to the MDS (Tables S3–S7). Analysis revealed several soil properties decreased across all treatments. Topsoil clay content, BD, SOC, SWC, NH₄⁺-N, and SSI decreased by 4.31%, 4.65%, 3.92%, 4.41%, 6.19%, and 12.51% respectively, with similar decreases observed in subsoil (Fig. 2a, c–e, h, i). Conversely, increases were observed in sand content, ECe, and pH by 11.33%, 16.43%, and 3.70% in the topsoil and 18.05%, 14.87%, and 8.76% in the subsoil, respectively (Fig. 2b, f, g). In conclusion, five consecutive years of cultivation have led to a decline in soil fertility for CK, as indicated by reductions in SOC, NH₄⁺-N and SSI, alongside an increase in pH, sand content and soil salinity (higher ECe). However, the HDI_{PM} treatment showed notable reductions in topsoil sand content and ECe compared to CK, suggesting that intensive irrigation under film mulching can

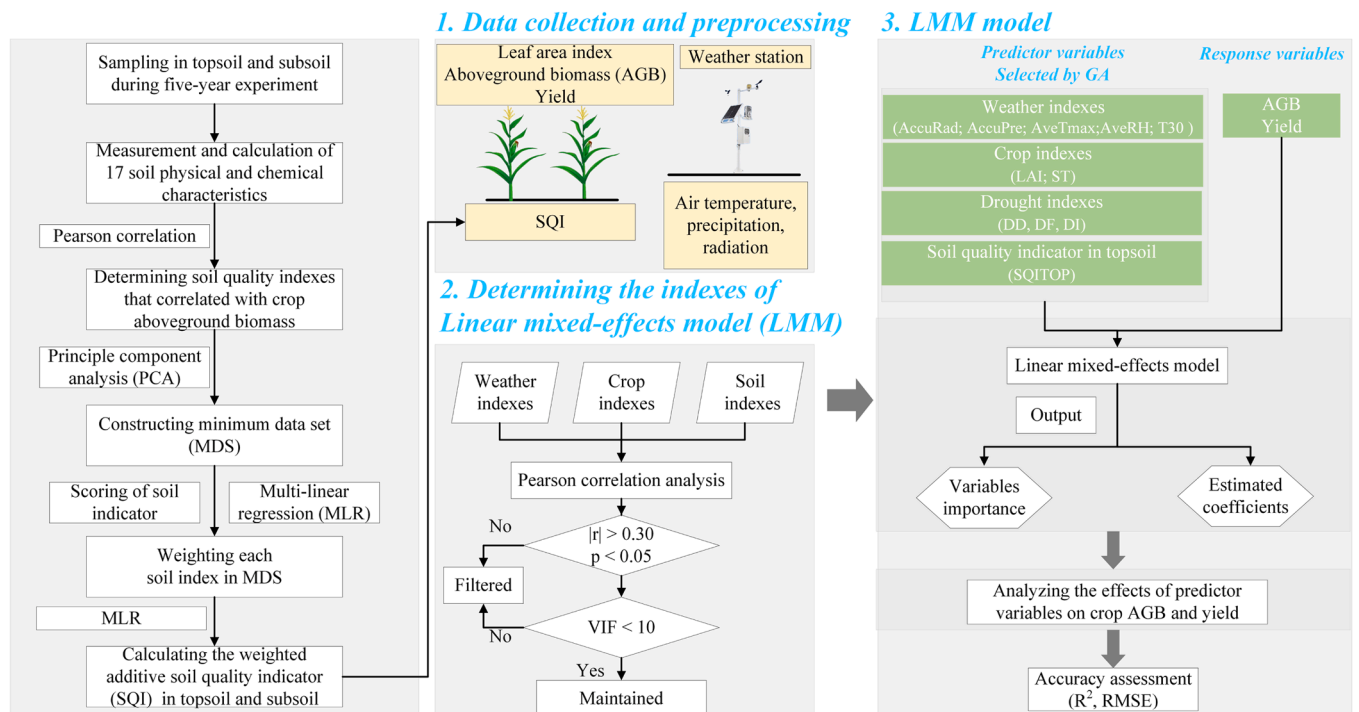


Fig. 1. Overview of the workflow to develop soil quality indicator (SQI) and the linear mixed-effects model (LMM) to estimate maize aboveground biomass and yield based on weather, crop, and soil characteristics. GA: genetic algorithm, R²: coefficient of determination, RMSE: root mean squared error.

Table 3
Descriptive statistics of soil property variables during the five-year experiment.

	Unit	Mean	Minimum	Maximum	Standard deviation	Coefficient of variation
Clay	%	23.14	19.89	27.13	1.48	6.39
Silt	%	66.81	58.45	75.17	4.87	7.29
Sand	%	14.04	6.02	20.53	2.38	16.93
BD	g cm ⁻³	1.37	1.23	1.54	0.06	4.51
FMC	cm ³ cm ⁻³	0.31	0.28	0.37	0.02	6.20
Ks	cm h ⁻¹	0.14	0.11	0.17	0.01	9.89
SWC	cm ³ cm ⁻³	0.23	0.19	0.29	0.02	8.42
ECe	dS m ⁻¹	6.90	4.28	9.64	1.38	20.06
pH	-	8.60	7.73	9.56	0.36	4.41
NO ₃ ⁻ -N	mg kg ⁻¹	5.99	3.02	9.71	2.32	38.82
NH ₄ ⁺ -N	mg kg ⁻¹	8.67	6.98	11.25	0.88	9.42
SOC	g kg ⁻¹	3.89	3.27	4.56	0.42	10.83
SP	%	48.09	41.89	53.28	2.27	4.71
TN	g kg ⁻¹	0.72	0.56	0.93	0.09	12.85
AP	mg kg ⁻¹	4.73	2.44	7.24	1.67	35.31
AK	mg kg ⁻¹	74.47	58.92	93.76	8.58	11.52
SSI	%	0.74	0.51	0.95	0.13	17.53

Note: bulk density (BD); field capacity (FMC); saturated hydraulic conductivity (Ks); soil water content before sowing (SWC); electrical conductivity of saturated extract (ECe); soil acidity (pH); soil nitrate-nitrogen (NO₃⁻-N); soil ammonium-nitrogen (NH₄⁺-N); soil organic carbon (SOC); soil porosity (SP); total nitrogen (TN); available phosphorus (AP); available potassium (AK); structural stability index (SSI).

mitigate certain aspects of soil degradation.

Excluding the HDI_{PM} treatment in topsoil, the SQI for both topsoil (SQITOP) and subsoil (SQISUB) across all treatments showed a decreasing trend over the years, as depicted in Fig. 3. Compared to initial values in 2016, by 2020, SQITOP decreased by 69.49 % for the CK, 24.24 % for BI_{PM}, 3.54 % for HDI_{PM}, 34.30 % for MDI_{PM}, and 53.14 % for LDI_{PM} treatments. Concurrently, SQISUB experienced reductions of 37.70 % for CK, 19.91 % for BI_{PM}, 7.70 % for HDI_{PM}, 22.64 % for MDI_{PM}, and 45.12 % for LDI_{PM} within the same period.

3.2. Final AGB, yield, IWP, and PFPN variation

Throughout the five-year periods, both the average crop yield and final AGB across all treatments showed a declining trend (Fig. 4a, b). The BI_{PM} treatment consistently outperformed the CK in terms of final AGB and yield annually (Fig. 4). Specifically, compared with CK, the BI_{PM} treatment showed increases of 30.94 % in mean yields and 76.41 % in final AGB. Furthermore, as the volume of irrigation increased, the average yield and final AGB from the drip irrigation treatments significantly improved. Compared to CK, HDI_{PM} increased average yield by 53.84 % and final AGB by 105.56 %; MDI_{PM} increased average yield by 43.85 % and final AGB by 92.52 %, while LDI_{PM} increased average yield by 3.19 % and final AGB by 59.54 %. IWP and PFPN trends also decreased over time (Fig. 4c and d). The average IWP and PFPN over multiple years increased significantly for BI_{PM}, HDI_{PM}, MDI_{PM}, and LDI_{PM} treatments by 26.28 % and 57.75 %, 85.11 % and 96.63 %, 156.18 % and 83.86 %, 268.54 % and 32.43 %, respectively, compared to CK, despite overall declines in IWP and PFPN from 2016 to 2020.

3.3. Grain yields, IWP, PFPN as affected by soil quality

The analysis revealed that as soil quality diminished, the efficacy of mulching in improving yield, IWP and PFPN also declined (Fig. 5a). The regression analysis showed slopes of 4.42 t ha⁻¹ for CK, 7.75 t ha⁻¹ for BI_{PM}, 34.13 t ha⁻¹ for HDI_{PM}, 49.51 t ha⁻¹ for MDI_{PM}, and 6.15 t ha⁻¹ for LDI_{PM} (Fig. 5a). Additionally, both IWP and PFPN

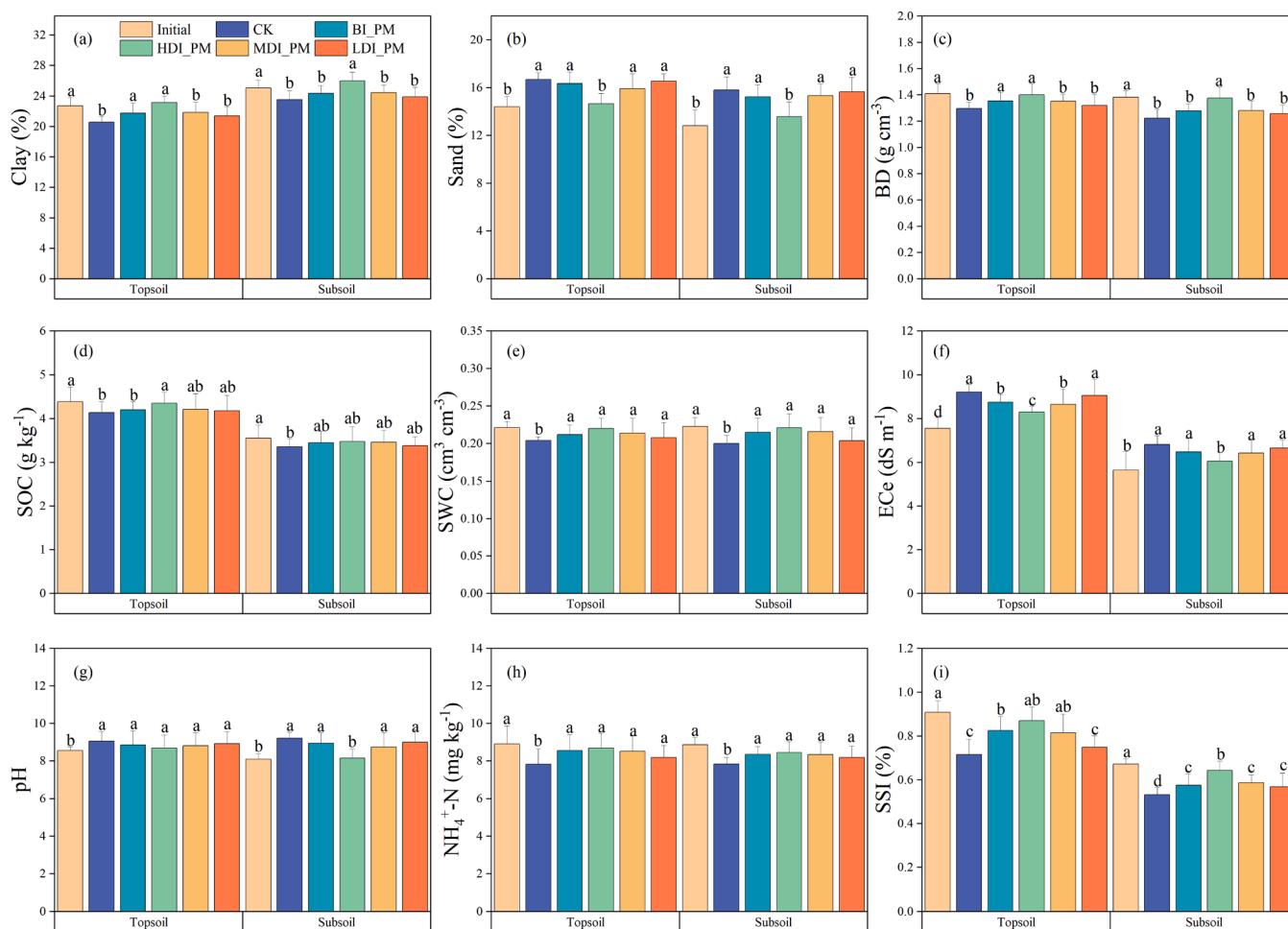


Fig. 2. Nine soil property indices were selected as the minimum soil dataset for the soil quality index, based on different irrigation treatments from 2016 (initial condition) to 2020 in topsoil (0–30 cm depth) and subsoil (30–60 cm depth). Lowercase letters denote comparisons of soil properties within 2020 and initial values, with no significant differences between means sharing the same letter ($p < 0.05$). BD is soil bulk density; SOC is soil organic carbon; SWC is soil water content; ECe is the electrical conductivity of saturated extract; pH is soil acidity; $\text{NH}_4^+\text{-N}$, soil ammonium-nitrogen; SSI is soil structural stability index. Treatments include border irrigation without mulching (CK); border irrigation with mulching (BI_PM); high irrigation level drip irrigation (HDI_PM); medium irrigation level drip irrigation (MDI_PM); low irrigation level drip irrigation (LDI_PM).

demonstrated significant positive associations with SQI (Fig. 5b and c). Film mulching treatments, in particular, contributed to a faster decline in IWP and PFPN than the CK treatment, as indicated by their relatively steep slopes.

3.4. Linear mixed-effects model

The model identified fixed effects—AccuRad, AccuPre, AveRH, T30, LAI, ST, DF, DI, and SQITOP—which accounted for at least 72 % ($R_m^2 = 0.72$) of the variability in AGB, with the overall model explaining up to 91 % of the variance ($R_c^2 = 0.91$), as shown in Table 4. Analysis revealed positive correlations of AccuRad, AccuPre, LAI, and SQITOP with AGB, whereas AveRH, T30, ST, DF, and DI were negatively correlated, as detailed in Table 4. Notably, AccuRad and AccuPre were significant contributors to AGB variance (Table 5). SQIs accounted for less than 5 % of AGB variation, with yearly random effects contributing between 0.2 % and 21.0 %. For yield estimation, both fixed (R_m^2) and total effects (R_c^2) demonstrated robustness, with values exceeding 75 %. Only the LAI and SQITOP exhibited positive correlations with yield in the LMM model (Table 4). Table 5 highlights LAI as the most crucial variable (importance ranging from 12.5–59.4 %), followed by SQITOP (6.4–32.1 %), and others.

3.5. Nonlinear relationships between maize yield and covariates

Fig. 6 elucidates the differential impact of six key variables on maize yield, as identified by the RF model. DI emerged as the paramount factor, contributing to 41.0 % of the yield variability, succeeded by LAI at 29.3 %, SQITOP at 17.9 %, AveTmax at 7.1 %, DF at 3.4 %, and T30 at 1.3 %. The model indicated a gradual decline in yield with the escalation of DI, AveTmax, DF, and T30 values (Fig. 6a, d, e, f). Conversely, a positive correlation was observed between LAI and yield (Fig. 6b), showcasing a notable yield enhancement when LAI surpassed 3, with yields stabilizing upon reaching an LAI of 4.5. Additionally, yields demonstrated a continuous decline with diminishing SQITOP values below 0.43, yet stabilized for SQITOP values above this threshold (Fig. 6c).

4. Discussion

4.1. Effects of film mulching and irrigation practices on soil quality

Continuous cultivation without incorporating external organic matter has been shown to compromise soil structure, diminish soil fertility, and ultimately lead to decreased crop yields, as evidenced by Raiesi and Beheshti (2022) and Sione et al. (2017). Independent of the specific

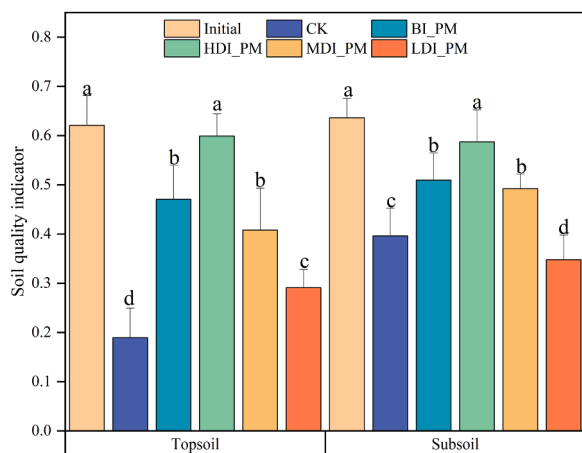


Fig. 3. Soil quality indicator values for topsoil and subsoil weighted by nine soil property indices from 2016 (initial) to 2020. Lowercase letters denote comparisons of soil properties within 2020 and initial values, with no significant differences between means sharing the same letter ($p < 0.05$). Topsoil is 0–30 cm soil depth; subsoil is 30–60 cm soil depth; border irrigation without mulching (CK); border irrigation with mulching (BI_PM); high irrigation level drip irrigation (HDI_PM); medium irrigation level drip irrigation (MDI_PM); low irrigation level drip irrigation (LDI_PM).

mulching and irrigation techniques applied, a marked increase in sand content, pH, and Ece was observed in both the topsoil and subsoil layers from 2016 to 2020 (see Fig. 2b, f, g and Table 3). This trend is mainly

attributable to the accumulation of sand and salts from irrigation water, corroborating findings from Zhang et al. (2021). Over five years, notable declines in clay content, BD, NH_4^+ , SSI, and SOC storage were recorded across all treatment groups (Fig. 2, Table S8), illustrating the adverse impacts of continuous cropping. Specifically, (1) the reduction in SOC undermines soil structure by impairing clay mineral flocculation, leading to decreases in clay content, BD, and SSI (Zhang et al., 2014; 2008), and (2) excessive irrigation promotes nutrient leaching, diminishing NH_4^+ levels (Dong et al., 2018). However, plastic film mulching was found to enhance SWC and NH_4^+ concentrations, as well as SSI in the subsoil, by the experiment’s conclusion, aligning with the outcomes of similar studies (Wang et al., 2023; Zhang et al., 2008). Moreover, HDI_PM was observed to alleviate the rising trends of sand content and salinity associated with film mulching (Fig. 2b and f). The concluding measurements of topsoil and subsoil AP and AK in 2020 fell below the optimal thresholds for maize growth, as Li et al. (2020) indicated, suggesting a need for targeted fertilizer application. Consequently, mulching not only mitigates the depletion of SOC and nutrients but also contributes positively to soil structural integrity and stability. Furthermore, employing irrigation water with low salinity and sand content, supplemented with potassium and phosphorus fertilizers, emerges as a viable approach for enhancing soil quality and fulfilling the nutritional demands of crops, as supported by Zhu et al. (2022).

Recent research highlights the significant influence of soil depth on SQI, aligning with the outcomes observed in our investigation (Li et al., 2022; Zhang et al., 2022b). Except the HDI_PM, subsoil consistently exhibited higher average SQI values compared to topsoil (Fig. 3). This distinction is mainly attributable to the sustained effects of irrigation and fertilizer management on the topsoil’s water and nutrient

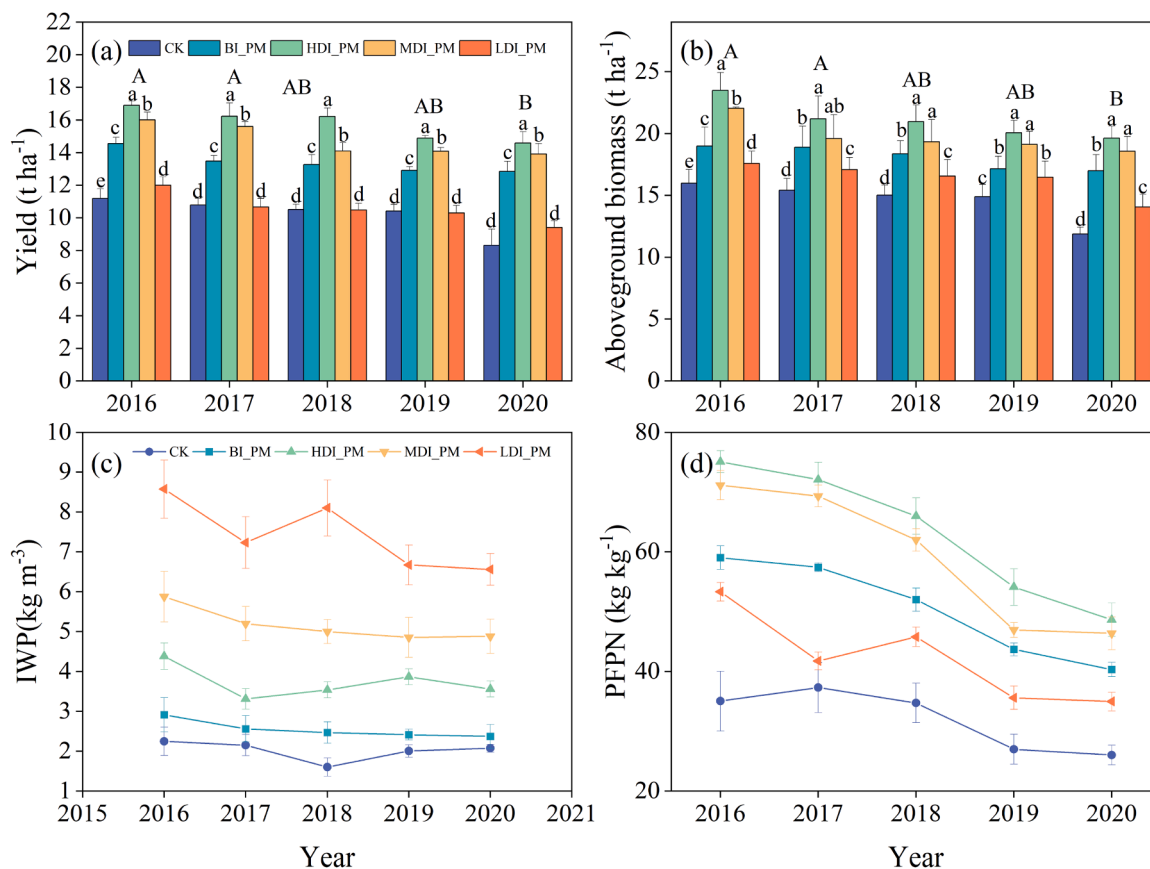


Fig. 4. Spring maize yield, aboveground biomass, irrigation water productivity (IWP), and partial factor productivity of nitrogen (PPFN) from 2016 to 2020 under different treatments. Uppercase letters denote comparisons of average yields of different treatments between multiple years. Lowercase letters denote comparisons of yields within a specific year. Means with the same letters do not significantly differ ($p < 0.05$). Border irrigation without mulching (CK); border irrigation with mulching (BI_PM); high irrigation level drip irrigation (HDI_PM); medium irrigation level drip irrigation (MDI_PM); low irrigation level drip irrigation (LDI_PM).

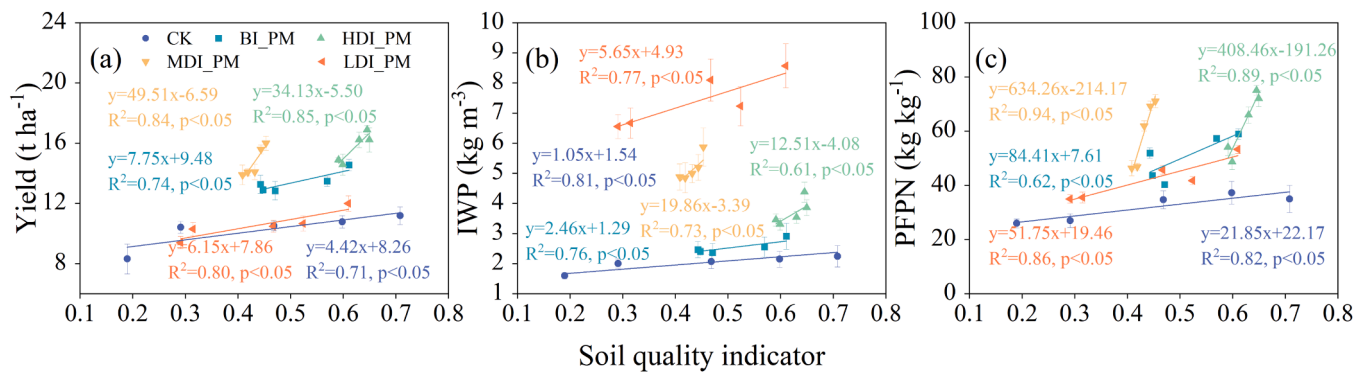


Fig. 5. Regression between the soil quality indicators and yield, irrigation water productivity (IWP), and partial factor productivity of nitrogen (PFPN) in all the treatments in the topsoil across five years. Border irrigation without mulching (CK); border irrigation with mulching (BI_PM); high irrigation level drip irrigation (HDI_PM); medium irrigation level drip irrigation (MDI_PM); low irrigation level drip irrigation (LDI_PM).

Table 4

Estimate of coefficients (β) and p-values in the linear mixed-effects model for predicting biomass and yield with selected variables.

Model source	Aboveground biomass			Model source	Yield		
	Estimated (β , t ha ⁻¹)	SE	p-value		Estimated (β , t ha ⁻¹)	SE	p-value
Fixed effects				Fixed effects			
Intercept	9.376 × 10 ⁻¹⁶	0.224	–	Intercept	2.942 × 10 ⁻¹⁶	0.0581	–
AccuRad	0.928	0.0726	***	AveTmax	-0.3737	0.143	*
AccuPre	0.0662	0.0714	*	T30	-0.101	0.120	*
AveRH	-0.130	0.0903	*	LAI	0.353	0.114	*
T30	-0.141	0.0433	**	DF	-0.218	0.0949	*
LAI	0.126	0.0543	*	DI	-0.192	0.0907	*
ST	-0.0993	0.0909	*	SQITOP	0.0827	0.0956	*
DF	-0.0877	0.0363	*				
DI	-0.1136	0.0363	***				
SQITOP	0.0804	0.0324	*				
R _m ²	0.72	–	–	R _m ²	0.76	–	–
Random effects				Random effects			
Year	0.247	0.498	–	Year	0.0535	0.248	–
Residual	0.0898	0.299	–	Residual	0.284	0.533	–
Deviance	64.3	–	–	Deviance	31.3	–	–
R _c ²	0.91	–	–	R _c ²	0.82	–	–

Note:
 *** p < 0.001;
 ** p < 0.01;
 * p < 0.05; ns = p > 0.05; R_m²: marginal coefficient of determination for fixed factors alone; R_c²: conditional coefficient of determination for fixed and random factors; SD: standard deviation. AccuRad: accumulative daily input radiation at different growth stages; AccuPre: accumulative daily precipitation at different growth stages; AveRH: average daily relative humidity at different growth stages; AveTmax: average maximum daily air temperature during the entire growth period; T30: accumulative high-temperature days (> 30 °C) at different growth stages/entire growth period; LAI: plant leaf area index at different growth stages/maximum values during the entire growth period; ST: plant stem thickness at different growth stages; DF: drought event frequency at different growth stages/total accumulation values during the entire growth period; DI, drought event intensity at the different growth stages/maximum value during the entire growth period; SQITOP: soil quality indicator in topsoil.

availability, its physical structure, and overall soil health, including issues such as salinization and loss of SOC (Gong et al., 2015; Molaeinasab et al., 2018). The decline in SQI noted in our study primarily resulted from reductions in SOC and the SSI (Fig. 2). Improvements in subsoil SQI were linked to two primary factors: (1) an increase in sand content, which bolsters soil permeability and facilitates the downward movement of irrigation water and nutrients (Zhang et al., 2021), and (2) enhanced SWC, which optimizes the water environment in the root zone, thereby supporting crop development (Chen et al., 2022). Notably, our analysis revealed no significant changes in SQI for the HDI_PM treatment in both topsoil and subsoil. This suggests that the strategic application of HDI_PM irrigation does not compromise soil quality for the sake of yield enhancement, offering a viable alternative to conventional local management approaches. However, even with the optimal HDI_PM treatment, yield, IWP, PFPN and SOC showed a decreasing trend over multiple years. This may be attributed to: (1) successive years of monoculture, which increase maize’s susceptibility to disease

pressure and limit biomass accumulation (Gentry et al., 2013); (2) the combination of high temperatures and sufficient water supply from drip irrigation in the study area, which created conditions conducive to SOC decomposition, leading to reduced soil SOC content without the addition of exogenous organic materials (Feng et al., 2024); and (3) increased ECe, which hinders crop absorption of water and nutrients, ultimately lowering yields (Zhang et al., 2021). In general, we recommend the adoption of drip irrigation in similar arid irrigation areas worldwide to achieve high yields and enhance water and fertilizer use efficiency. Additionally, exploring diversified cropping patterns, such as fallow and crop rotation, can promote land restoration. It is also important to investigate the use of green manure and organic matter to maintain and potentially improve soil quality, thereby ensuring high-yield and sustainable agriculture.

Table 5
Variable importance derived from linear mixed-effect models for maize aboveground biomass and yield.

LMM Predictors	Aboveground biomass			LMM Predictors	Yield		
	RIV	Lower	Upper		RIV	Lower	Upper
Fixed effects				Fixed effects			
AccuRad	39.3	11.5	76.1	AveTmax	5.1	1.7	10.3
AccuPre	20.1	3.2	40.5	T30	6.6	2.4	12.4
AveRH	9.2	1.2	25.1	LAI	42.3	12.5	59.4
T30	4.1	2.5	5.2	DF	10.1	2.7	15.0
LAI	6.3	0.9	18.2	DI	15.1	1.9	30.9
ST	7.3	0.3	24.4	SQITOP	20.8	6.4	32.1
DF	8.2	0.2	28.0				
DI	1.4	0.0	4.3				
SQITOP	4.1	1.3	6.5				
Random effects				Random effects			
Year	6.0	0.2	21.0	Year	7.3	2.7	15.0
Statistical indicators				Statistical indicators			
R ²	0.91	-	-	R ²	0.82	-	-
RMSE	0.23	-	-	RMSE	0.45	-	-

Note: RIV: relatively important variables, R²: coefficients of determination, RMSE: root mean square error. AccuRad: accumulative daily input radiation at different growth stages; AccuPre: accumulative daily precipitation at different growth stages; AveRH: average daily relative humidity at different growth stages; AveTmax: average maximum daily air temperature during the entire growth period; T30: accumulative high-temperature days (> 30 °C) at different growth stages/entire growth period; LAI: plant leaf area index at different growth stages/maximum values during the entire growth period; ST: plant stem thickness at different growth stages; DF: drought event frequency at different growth stages/total accumulation values during the entire growth period; DI, drought event intensity at the different growth stages/maximum value during the entire growth period; SQITOP: soil quality indicator in topsoil.

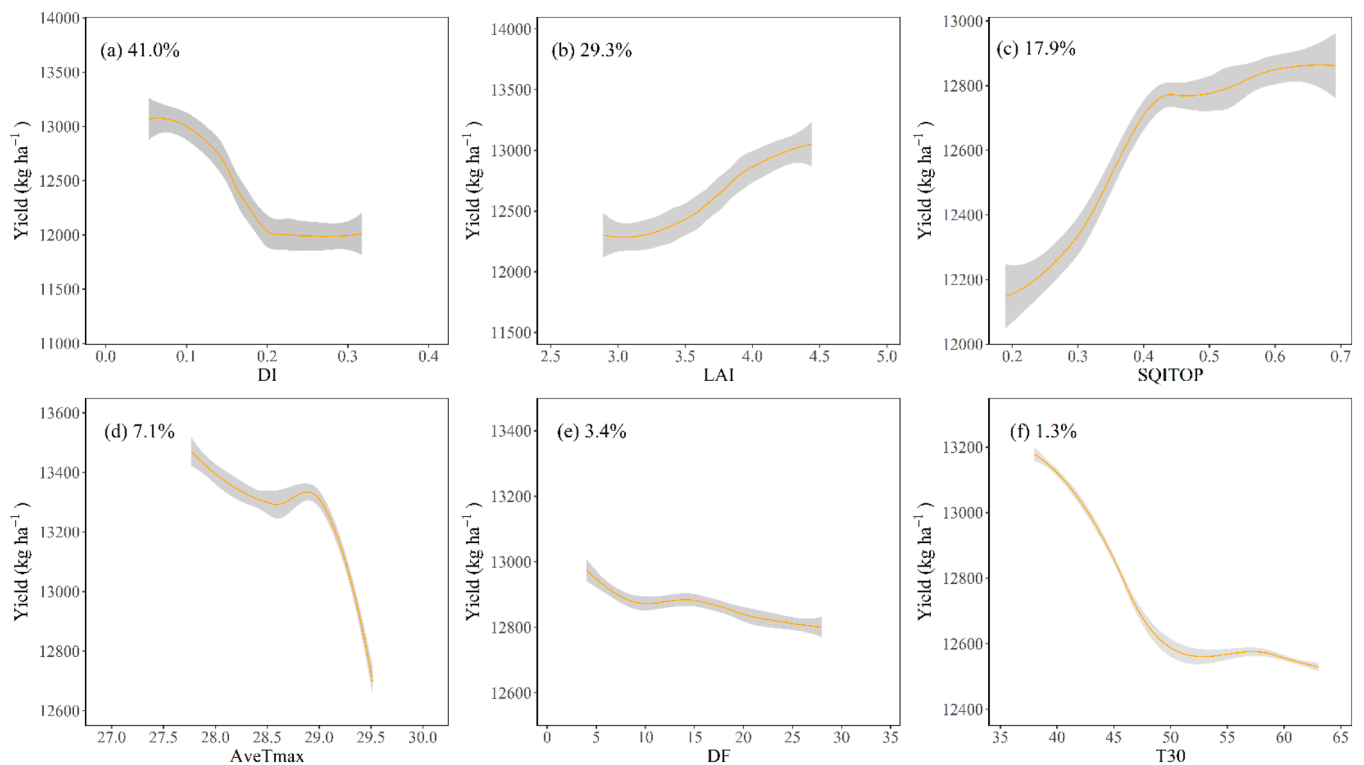


Fig. 6. Partial dependence of crop yield on six explanatory variables. (a) maximum drought event intensity during the entire growth period, DI; (b) maximum plant leaf area index during the entire period, LAI; (c) soil quality indicator in topsoil, SQITOP; (d) average daily maximum temperature during the entire period, AveTmax; (e) total accumulation of drought event frequency during the entire period, DF; (f) total accumulation of accumulative high-temperature days (> 30°C) during the entire period, T30. The percentage value in each plot represents the relative importance of each predictor variable based on the random forest model. Gray shaded areas indicate the 95 % confidence intervals.

4.2. Maize yield change in response to SQI

Our analysis revealed that over five growing seasons, mean yields experienced significant increases for mulching treatments, compared to the CK (Fig. 4). And, yields for BI_PM were outpaced by HDI_PM, suggesting that drip irrigation more effectively satisfies crop water needs and fosters a conducive root environment by enhancing root growth and

soil nutrient accessibility, thereby potentially boosting yield (Chen et al., 2021). Additionally, drip irrigation treatments demonstrated superior IWP and PFPN relative to CK, aligning with observations by Zhang et al. (2021). These treatments minimize water evaporation, optimize the evaporation-transpiration ratio, encourage root proliferation, and influence soil nutrient distribution (Wang et al., 2018, 2020a), making drip irrigation a more efficient alternative to extensive border irrigation

practices. Furthermore, regression analyses confirmed positive correlations between grain yields, IWP, PFPN, and SQITOP (Fig. 5). The deterioration in yield alongside declining soil quality was linked to diminished water and nitrogen use efficiencies (Fig. 2). Moreover, incremental increases in irrigation water inputs over the years could lead to enhanced water leakage and nutrient leaching (Table S1), thereby restricting nutrient availability in the soil (Singh et al., 2020), which emerged as an additional yield limiting factor.

4.3. Nonlinear relationship between dominant factors and maize yield

The RF model identified DI as the paramount variable impacting maize yield, with LAI and SQITOP following in importance, as depicted in Fig. 6. DI and DF exerted a negative influence on yield, underscoring their critical role in the formation of yield and the variable susceptibility of crops to drought at different stages of growth (Monteleone et al., 2022). In particular, drought events during critical periods such as flowering and grain-filling were found to be significantly detrimental to crop yield (Yu et al., 2018a, 2018b). Additionally, the analysis showed that extreme temperature metrics, including AveTmax and T30, adversely affected maize yield (Figs. 6d and 6f). SQITOP, contributing 17.9 % to the model's importance (Fig. 6), underscored the potential of adequate irrigation strategies to mitigate adverse effects of reduced soil quality, especially concerning water retention, on yield. Furthermore, the application of high fertilizer inputs was demonstrated to alleviate the limitations posed by soil fertility in irrigated conditions (Zhang et al., 2020).

The RF model's partial dependence plots identified critical threshold values for variables impacting maize yield. Notably, the yield appeared to stabilize when the LAI exceeded 4.5. Furthermore, yield stability was observed when the SQITOP was higher than 0.43, as illustrated in Fig. 6c. This stability is likely due to the high-quality soil's ability to maintain a consistently moist environment, attributable to its superior water retention capacity (Fan et al., 2022). Conversely, a SQITOP below 0.43 led to a proportional decrease in yield, associated with an increase in sand content and a deterioration of soil structure (Fig. 2b and i), which enhances water conductivity and potentially facilitates groundwater recharge to the topsoil. However, this process also elevates soil salinity (as evidenced by increased ECe in Fig. 2f), promoting soil salinization (Zhang et al., 2021). Considering the significant role of drought as a yield-limiting factor, we advocate for the adoption of drip irrigation at a soil matric potential of -10 kPa. This approach aims to optimize soil moisture levels, mitigate drought stress, and ultimately enhance maize yield.

4.4. Research limitations

This investigation encountered several limitations. Primarily, the dataset was confined to observations from a single site over five years, potentially limiting our findings' generalizability across diverse agricultural contexts. Future research should extend to multiple locations to assess the broader impacts of climate change and soil property variations on crop productivity over extended periods. Secondly, soil property measurements were conducted solely at harvest each year, necessitating more frequent assessments throughout critical maize growth phases to capture SQI dynamics better. Thirdly, the study employed linear scoring and multiple linear regression techniques to assess and calculate the SQI within the MDS. Recent advancements suggest that nonlinear scoring functions and innovative network analysis approaches may offer more accurate depictions of the interplay between plant growth and soil conditions (Chen et al., 2023; Martín-Sanz et al., 2022). Hence, there is a pressing need to explore alternative weighting methodologies further to more precisely ascertain soil quality fluctuations across varied agricultural areas.

5. Conclusions

We found that the SQI in both topsoil and subsoil decreased after five years, except for the HDI_{PM} treatment, in the arid irrigation region. This decline was primarily due to a decrease in SOC and structural stability, as well as an increase in sand content and soil salinity. Additionally, LMM incorporating weather, drought, and soil properties were developed to predict maize biomass and yield. The RF model also indicated SQITOP as an important variable affecting yield, with a threshold was 0.43. Overall, we recommend using drip irrigation based on a soil matric potential of -10 kPa to maximize maize yield and PFPN, while also mitigating the decline in the SQI in the Hetao irrigation region. Given the declining trend in soil quality observed over five years of continuous experiments, it is imperative to investigate the potential of alternative agronomic practices for future agricultural production. Such practices may include the incorporation of green manure and organic matter combined with drip irrigation to achieve high yields and maintain soil fertility for sustainable agriculture, while avoiding drought stress and soil quality limitations.

CRedit authorship contribution statement

Hao Quan: Writing – review & editing, Writing – original draft, Visualization, Validation, Software, Investigation, Data curation. **Lihong Wu:** Writing – review & editing, Methodology, Formal analysis, Data curation. **Kadambot H.M. Siddique:** Writing – review & editing, Methodology, Investigation, Formal analysis. **Hao Feng:** Writing – review & editing, Supervision, Methodology, Funding acquisition, Conceptualization. **Bin Wang:** Writing – review & editing, Validation, Supervision, Methodology, Investigation, Formal analysis, Conceptualization. **Lianhai Wu:** Writing – review & editing, Investigation, Data curation, Conceptualization. **Jiaming Sun:** Investigation, Data curation. **Tibin Zhang:** Writing – review & editing, Supervision, Methodology, Formal analysis, Data curation.

Declaration of Competing Interest

The authors declare that they have no known competing financial interests or personal relationships that could have appeared to influence the work reported in this paper.

Acknowledgments

This work was jointly supported by the National Key R&D Program of China (2021YFD1900700) and the National Natural Science Foundation of China (Grant Nos. 51879224 and 51609237).

Appendix A. Supporting information

Supplementary data associated with this article can be found in the online version at doi:10.1016/j.agwat.2024.109221.

Data availability

Data will be made available on request.

References

- Amgain, N.R., Xu, N., Rabbany, A., Fan, Y., Bhadha, J.H., 2022. Developing soil health scoring indices based on a comprehensive database under different land management practices in Florida. *Agrosyst. Geosci. Environ.* 5 (3), e20304.
- Bao, S.D., 2000. *Soil Agricultural-Chemical Analysis*. China Agric. Press, Beijing.
- Breiman, L., 2001. Random forests. *Mach. Learn.* 45, 5–32.
- Chen, N., Li, X., Shi, H., Hu, Q., Zhang, Y., Leng, X., 2021. Effect of biodegradable film mulching on crop yield, soil microbial and enzymatic activities, and optimal levels of irrigation and nitrogen fertilizer for the *Zea mays* crops in arid region. *Sci. Total Environ.* 776, 145970.

- Chen, S., Mao, X., Shang, S., 2022. Response and contribution of shallow groundwater to soil water/salt budget and crop growth in layered soils. *Agric. Water Manag.* 266, 107574.
- Chen, X., Zhang, X., Wei, Y., Zhang, S., Cai, C., Guo, Z., Wang, J., 2023. Assessment of soil quality in a heavily fragmented micro-landscape induced by gully erosion. *Geoderma* 431, 116369.
- De Cárcer, P.S., Sinaj, S., Santonja, M., Fossati, D., Jeangros, B., 2019. Long-term effects of crop succession, soil tillage and climate on wheat yield and soil properties. *Soil Tillage Res* 190, 209–219.
- Ding, D., Feng, H., Zhao, Y., Hill, R.L., Yan, H., Chen, H., Hou, H., Chu, X., Liu, J., Wang, N., Zhang, T., Dong, Q., 2019. Effects of continuous plastic mulching on crop growth in a winter wheat-summer maize rotation system on the Loess Plateau of China. *Agric. For. Meteorol.* 27, 385–397.
- Dong, Q., Yang, Y., Zhang, T., Zhou, L., He, J., Chau, H.W., Zou, Y., Feng, H., 2018. Impacts of ridge with plastic mulch-furrow irrigation on soil salinity, spring maize yield and water use efficiency in an arid saline area. *Agric. Water Manag.* 201, 268–277.
- Fan, Y., He, L., Liu, Y., Wang, S., 2022. Optimal cropping patterns can be conducive to sustainable irrigation: Evidence from the drylands of Northwest China. *Agric. Water Manag.* 274, 107977.
- Feng, Z., Miao, Q., Shi, H., Li, X., Yan, J., Gonçalves, J.M., Dai, L., Feng, W., 2024. Irrigation scheduling in sand-layered farmland: evaluation of water and salinity dynamics in the soil by SALTMED-1D model under mulched maize production in Hetiao Irrigation District, China. *Eur. J. Agron.* 157, 127177.
- Fernández, J.E., Alcon, F., Diaz-Espejo, A., Hernandez-Santana, V., Cuevas, M.V., 2020. Water use indicators and economic analysis for on-farm irrigation decision: a case study of a super high density olive tree orchard. *Agric. Water Manag.* 237, 106074.
- Foley, J.A., Ramankutty, N., Brauman, K.A., Cassidy, E.S., Gerber, J.S., Johnston, M., Mueller, N.D., O'Connell, C., Ray, D.K., West, P.C., Balzer, C., Bennett, E.M., Carpenter, S.R., Hill, J., Monfreda, C., Polasky, S., Rockström, J., Sheehan, J., Siebert, S., Tilman, D., Zaks, D.P.M., 2011. Solutions for a cultivated planet. *Nature* 478 (7369), 337–342.
- Gan, F., Shi, H., Yan, Y., Pu, J., Dai, Q., Gou, J., Fan, Y., 2024. Soil quality assessment of karst trough valley under different bedrock strata dip and land-use types, based on a minimum data set. *Catena* 241, 108048.
- Gao, H., Yan, C., Liu, Q., Ding, W., Chen, B., Li, Z., 2019. Effects of plastic mulching and plastic residue on agricultural production: a meta-analysis. *Sci. Total Environ.* 651, 484–492.
- Gentry, L.F., Ruffo, M.L., Below, F.E., 2013. Identifying factors controlling the continuous corn yield penalty. *Agron. J.* 105, 295–303.
- Gong, L., Ran, Q., He, G., Tiyip, T., 2015. A soil quality assessment under different land use types in Keriya river basin, Southern Xinjiang, China. *Soil Tillage Res.* 146, 223–229.
- Guo, Q., Huang, G., Guo, Y., Zhang, M., Zhou, Y., Duan, L., 2021. Optimizing irrigation and planting density of spring maize under mulch drip irrigation system in the arid region of Northwest China. *Field Crops Res.* 266, 108141.
- Jiang, X.J., Liu, W.J., Wang, E.H., Zhou, T.Z., Xin, P., et al., 2017. Residual plastic mulch fragments effects on soil physical properties and water flow behavior in the Minqin Oasis, northwestern China. *Soil Tillage Res.* 166 (1), 100–107.
- Karlen, D.L., Gardner, J.C., Rosek, M.J., 1998. A soil quality framework for evaluating the impact of CRP. *J. Prod. Agric.* 11, 56–60.
- Klute, A., Dirksen, C., 1986. *Hydraulic Conductivity of Saturated Soils*. ASA and SSSA, Madison, Wisconsin, USA.
- Li, Y.Z., Hu, Y.C., Song, D.P., Liang, S.H., Qin, X.L., Siddique, H.M., 2019. The effects of straw incorporation with plastic film mulch on soil properties and bacterial community structure on the loess plateau. *Eur. J. Soil Sci.* 72 (2), 979–994.
- Li, Z., Liu, Z., Zhang, M., Li, C., Li, Y.C., Wan, Y., Martin, C.G., 2020. Long-term effects of controlled-release potassium chloride on soil available potassium, nutrient absorption and yield of maize plants. *Soil Tillage Res.* 196, 104438.
- Li, Y., Ming, B., Fan, P., Liu, Y., Wang, K., Hou, P., Xue, J., Li, S., Xie, R., 2022. Quantifying contributions of leaf area and longevity to leaf area duration under increased planting density and nitrogen input regimens during maize yield improvement. *Field Crops Res.* 283, 108551.
- Li, L., Wang, B., Feng, P., Wang, H., He, Q., Wang, Y., Liu, D.L., Li, Y., He, J., Feng, H., Yang, G., Yu, Q., 2021. Crop yield forecasting and associated optimum lead time analysis based on multi-source environmental data across China. *Agric. For. Meteorol.* 308–309, 108558.
- Li, S., Wang, B., Liu, D., Chen, C., Feng, P., Huang, M., Wang, X., Shi, L., Waters, C., Huete, A., Yu, Q., 2023. Can agronomic options alleviate the risk of compound drought-heat events during wheat flowering period in southeastern Australia? *Eur. J. Agron.* 153, 127030.
- Luo, Z., Gan, Y., Niu, Y., Zhang, R., Li, L., Cai, L., Xie, J., 2017. Soil quality indicators and crop yield under long-term tillage systems. *Exp. Agric.* 53 (4), 497–511.
- Luo, S., Zhu, L., Liu, J., Bu, L., Yue, S., Shen, Y., Li, S., 2015. Sensitivity of soil organic carbon stocks and fractions to soil surface mulching in semiarid farmland. *Eur. J. Soil Biol.* 67, 35–42.
- Ma, X., He, Q., Zhou, G., 2018. Sequence of changes in maize responding to soil water deficit and related critical thresholds. *Front Plant Sci.* 9, 511.
- Ma, Y., Liu, W., Qiao, Y., Qiao, W., Yang, H., Zhong, Y., Yang, H., Wang, H., Li, Y., Dong, B., Liu, M., 2023. Effects of soil salinity on foxtail millet osmoregulation, grain yield, and soil water utilization under varying water conditions. *Agric. Water Manag.* 284, 108354.
- Martín-Sanz, J.P., de Santiago-Martín, A., Valverde-Asenjo, I., Quintana-Nieto, J.R., González-Huecas, C., López-Lafuente, A.L., 2022. Comparison of soil quality indexes calculated by network and principal component analysis for carbonated soils under different uses. *Ecol. Indic.* 143, 109374.
- Meng, F., Dungait, J.A.J., Xu, X., Bol, R., Zhang, X., Wu, W., 2017. Coupled incorporation of maize (*Zea mays* L.) straw with nitrogen fertilizer increased soil organic carbon in Fluvic Cambisol. *Geoderma* 304, 19–27.
- Molaeinasab, A., Bashari, H., Tarkesh Esfahani, M., Mosaddeghi, M.R., 2018. Soil surface quality assessment in rangeland ecosystems with different protection levels, central Iran. *Catena* 171, 72–82.
- Monteleone, B., Borzì, I., Bonaccorso, B., Martina, M., 2022. Developing stage-specific drought vulnerability curves for maize: the case study of the Po River basin. *Agric. Water Manag.* 269, 107713.
- Montgomery, E.G., 1911. Correlation studies in corn. *Neb. Agric. Exp. Stn. Annu. Rep.* 24, 108–159.
- Munns, R., Tester, M., 2008. Mechanisms of salinity tolerance. *Annu. Rev. Plant Biol.* 59, 651–681.
- Nelson, D.W., Sommers, L.E., 1982. Total Carbon, Organic Carbon and Organic Matter (Soil Sci. Soc. Am. J., Inc.). In: Page, A.L., Miller, R.H., Keeney, D.R. (Eds.), *Methods of Soil Analysis, Part 2 Chemical and Microbiological Properties*. American Society of Agronomy, Inc., Madison, pp. 539–579 (Soil Sci. Soc. Am. J., Inc.).
- Nunes, M.R., Karlen, D.L., Veum, K.S., Moorman, T.B., 2020. A SMAF assessment of U.S. tillage and crop management strategies. *Environ. Sustain. Indic.* 8, 100072.
- Pieri, C.J.M.G., 1992. *Fertility of Soils: A Future for Farming in the West African Savannah*. Springer-Verlag, Berlin, Germany.
- Qi, Z., Feng, H., Zhao, Y., Zhang, T., Yang, A., Zhang, Z., 2018. Spatial distribution and simulation of soil moisture and salinity under mulched drip irrigation combined with tillage in an arid saline irrigation district, northwest China. *Agric. Water Manag.* 201, 219–231.
- Qi, Y., Ossowicki, A., Yang, X., Huerta-Lwanga, E., Dini-Andreote, F., Geissen, V., Garbeva, P., 2020. Effects of plastic mulch litter residues on wheat rhizosphere and soil properties. *J. Hazard. Mater.* 387, 121711.
- Qiao, L., Wang, X., Smith, P., Fan, J., Lu, Y., Emmett, B., Li, R., Dorling, S., Chen, H., Liu, S., Benton, T.G., Wang, Y., Ma, Y., Jiang, R., Zhang, F., Piao, S., Müller, C., Yang, H., Hao, Y., Li, W., Fan, M., 2022. Soil quality both increases crop production and improves resilience to climate change. *Nat. Clim. Chang.* 12 (6), 574–580.
- Quan, H., Wu, L., Ding, D., Yang, Z., Wang, N., Chen, G., Li, C., Dong, Q., Feng, H., Zhang, T., Siddique, K.H.M., 2022. Interaction between soil water and fertilizer utilization on maize under plastic mulching in an arid irrigation region of China. *Agric. Water Manag.* 265, 107494.
- Raiesi, F., Beheshti, A., 2022. Evaluating forest soil quality after deforestation and loss of ecosystem services using network analysis and factor analysis techniques. *Catena* 208, 105778.
- Rodrigues, G.C., Pereira, L.S., 2009. Assessing economic impacts of deficit irrigation as related to water productivity and water costs. *Biosyst. Eng.* 103, 536–551.
- Rojas, R.V., Achouri, M., Marouli, J., Caon, L., 2016. Healthy soils: a prerequisite for sustainable food security. *Environ. Earth Sci.* 75 (3), 180.
- Sadras, V.O., Milroy, S.P., 1996. Soil-water thresholds for the responses of leaf expansion and gas exchange: a review. *Field Crops Res.* 47 (2), 253–266.
- Salcedo, F.P., Cutillas, P.P., Cabañero, J.A., Vivaldi, A.G., 2022. Use of remote sensing to evaluate the effects of environmental factors on soil salinity in a semi-arid area. *Sci. Total Environ.* 815, 152524.
- Seconda, L., Fouillet, H., Huneau, J.-F., Pointereau, P., Baudry, J., Langevin, B., Lairon, D., Allès, B., Touvier, M., Hercberg, S., Mariotti, F., Kesse-Guyot, E., 2021. Conservative to disruptive diets for optimizing nutrition, environmental impacts and cost in French adults from the NutriNet-Santé cohort. *Nat. Food* 2 (3), 174–182.
- Singh, S., Bhattarai, R., Negm, L.M., Youssef, M.A., Pittelkow, C.M., 2020. Evaluation of nitrogen loss reduction strategies using DRAINMOD-DSSAT in east-central Illinois. *Agric. Water Manag.* 240, 106322.
- Sione, S.M.J., Wilson, M.G., Lado, M., González, A.P., 2017. Evaluation of soil degradation produced by rice crop systems in a Vertisol, using a soil quality index. *Catena* 150, 79–86.
- Teixeira, P.C., Donagemma, G.K., Fontana, A.L., Teixeira, W.G., 2017. *Manual de métodos de análise de solo EMBRAPA (Ed.)*, Embrapa Solos. Bras. DF. 573.
- Tong, W.-J., Chen, X.-L., Wen, X.-Y., Chen, F., Zhang, H., Chu, Q.-Q., Dikgwatlhe, S., 2015. Applying a salinity response function and zoning saline land for three field crops: a case study in the Hetiao Irrigation District, Inner Mongolia, China. *J. Integr. Agric.* 14 (1), 178–189.
- Vasu, D., Singh, S.K., Ray, S.K., Duraisami, V.P., Tiwary, P., Chandran, P., Nimkar, A.M., Anantwar, S.G., 2016. Soil quality index (SQI) as a tool to evaluate crop productivity in semi-arid Deccan plateau, India. *Geoderma* 282, 70–79.
- Wang, L., Li, X.G., Lv, J., Fu, T., Ma, Q., Song, W., Wang, Y.P., Li, F.-M., 2017. Continuous plastic-film mulching increases soil aggregation but decreases soil pH in semiarid areas of China. *Soil Tillage Res.* 167, 46–53.
- Wang, Y., Li, S., Qin, S., Guo, H., Yang, D., Lam, H.-M., 2020a. How can drip irrigation save water and reduce evapotranspiration compared to border irrigation in arid regions in northwest China. *Agric. Water Manag.* 239, 106256.
- Wang, J., Niu, W., Guo, L., Liu, L., Li, Y., Dyck, M., 2018. Drip irrigation with film mulch improves soil alkaline phosphatase and phosphorus uptake. *Agric. Water Manag.* 201, 258–267.
- Wang, Y., Pang, J., Zhang, M., Tian, Z., Wei, T., Jia, Z., Ren, X., Zhang, P., 2023. Is adding biochar be better than crop straw for improving soil aggregates stability and organic carbon contents in film mulched fields in semiarid regions? –evidence of 5-year field experiment. *J. Environ. Manag.* 338, 117711.
- Wang, Z., Shao, G., Lu, J., Zhang, K., Gao, Y., Ding, J., 2020b. Effects of controlled drainage on crop yield, drainage water quantity and quality: a meta-analysis. *Agric. Water Manag.* 239, 106253.
- Welikala, R.A., Fraz, M.M., Dehmeshki, J., Hoppe, A., Tah, V., Mann, S., Williamson, T. H., Barman, S.A., 2015. Genetic algorithm based feature selection combined with

- dual classification for the automated detection of proliferative diabetic retinopathy. *Comput. Med. Imaging Graph.* 43, 64–77.
- Yang, W., Feng, G., Miles, D., Gao, L., Jia, Y., Li, C., Qu, Z., 2020. Impact of biochar on greenhouse gas emissions and soil carbon sequestration in corn grown under drip irrigation with mulching. *Sci. Total Environ.* 729, 138752.
- Yang, L., Heng, T., He, X., Yang, G., Zhao, L., Li, Y., Xu, Y., 2023. Spatial-temporal distribution and accumulation characteristics of residual plastic film in cotton fields in arid oasis area and the effects on soil salt transport and crop growth. *Soil Tillage Res.* 231, 105737.
- Yu, C., Huang, X., Chen, H., Huang, G., Ni, S., Wright, J.S., Hall, J., Ciaia, P., Zhang, J., Xiao, Y., Sun, Z., Wang, X., Yu, L., 2018a. Assessing the impacts of extreme agricultural droughts in China under climate and socioeconomic changes. *Earth's Future* 6 (5), 689–703.
- Yu, H., Zhang, Q., Sun, P., Song, C., 2018b. Impact of droughts on winter wheat yield in different growth stages during 2001–2016 in Eastern China. *Int. J. Disaster Risk Sci.* 9, 376–391.
- Zhang, G.S., Chan, K.Y., Li, G.D., Huang, G.B., 2008. Effect of straw and plastic film management under contrasting tillage practices on the physical properties of an erodible loess soil. *Soil Tillage Res.* 98, 113–119.
- Zhang, F., Li, S., Yue, S., Song, Q., 2022a. The effect of long-term soil surface mulching on SOC fractions and the carbon management index in a semiarid agroecosystem. *Soil Tillage Res.* 216, 105233.
- Zhang, X., Qu, J., Li, H., La, S., Tian, Y., Gao, L., 2020. Biochar addition combined with daily fertigation improves overall soil quality and enhances water-fertilizer productivity of cucumber in alkaline soils of a semi-arid region. *Geoderma* 363, 114170.
- Zhang, P., Wei, T., Jia, Z.K., Han, Q.F., Ren, X.L., 2014. Soil aggregate and crop yield changes with different rates of straw incorporation in semiarid areas of northwest China. *Geoderma* 230, 41–49.
- Zhang, Y., Xia, C., Zhang, X., Sha, Y., Feng, G., Gao, Q., 2022b. Quantifying the relationships of soil properties and crop growth with yield in a NPK fertilizer application maize field. *Comput. Electron. Agric.* 198, 107011.
- Zhang, T., Zou, Y., Kisekka, I., Biswas, A., Cai, H., 2021. Comparison of different irrigation methods to synergistically improve maize's yield, water productivity and economic benefits in an arid irrigation area. *Agric. Water Manag.* 243, 106497.
- Zhao, J., Liu, Z., Lai, H., Zhao, M., Zhu, Q., Zhao, C., Yang, D., Li, X., 2023. The impacts of soil tillage combined with plastic film management practices on soil quality, carbon footprint, and peanut yield. *Eur. J. Agron.* 148, 126881.
- Zhu, W., Kang, Y., Li, X., Wan, S., Dong, S., 2022. Changes in understory vegetation during the reclamation of saline-alkali soil by drip irrigation for shelterbelt establishment in the Hetao Irrigation Area of China. *Catena* 214, 106247.